Challenging Glass Conference Proceedings – Volume 10 – June 2026 – Louter, Bos & Belis (Eds.)
International Conference on the Architectural and Structural Application of Glass
Challenging Glass Conference 10 – 15-17 June 2026 – TU Delft – The Netherlands

An Experimental Study on the Adhesion Performance of SSG Sealant to Timber and its Application in Mock-up Assemblies

Katsuta Tomoeda [a]

a ASAHI BUILDING-WALL CO., LTD., Japan, katsuto-tomoeda@agb.co.jp

Abstract

In recent years, the Japanese architectural industry has seen a growing trend toward timber construction, driven by increasing environmental awareness. However, despite the use of timber in structural elements, aluminium sash frames remain prevalent in many buildings. This study aims to develop a durable, all-timber sash system by focusing on the Structural Silicone Glazing (SSG) method. The method allows timber components to be used without direct exposure to outdoor conditions, thereby enhancing durability. This research investigates the adhesion performance of SSG sealant on timber. Initially, adhesion tests were conducted on various timber specifications to identify optimal candidates. Subsequently, residual adhesion performances were investigated on selected specimens pre-treated by several artificial aging methods. Experimental validation was performed using a full-scale specimen. A timber SSG unit (GW2940×GH805) was installed in a wind pressure chamber. The unit was subjected to 2.2 million cycles +1 kPa wind pressure, followed by a single application of ±4.5 kPa. After testing, the specimens were extracted from the unit for adhesion tests to assess residual performance. Additionally, full-scale mock-ups of arches and a circular shape were fabricated. CNC machining enabled the precise shaping of timber to match the edge curve of glass, which confirmed the feasibility of producing timber SSG units with complex geometries. These results demonstrate the feasibility of applying SSG to timber sash systems with appropriate material selection.

Keywords

SSG sealant, glass, Timber, Experiment, Mock-up

Article Information

- Digital Object Identifier (DOI): 10.47982/cgc.10.697
- Published by Challenging Glass, on behalf of the author(s), at Stichting OpenAccess.
- Published as part of the peer-reviewed Challenging Glass Conference Proceedings, Volume 10, June 2026, 10.47982/cgc.10
- Editors: Christian Louter, Freek Bos & Jan Belis

1. Introduction

In recent years, the Japanese building industry has seen a promotion of timber use driven by growing environmental awareness, leading to an increase in wooden and semi-wooden structures utilizing timber in their structural frameworks. However, for the window sashes in these buildings, conventional aluminum frames continue to be used in most cases. A primary concern regarding the use of timber in sashes is degradation resulting from environmental impacts such as wind, rain, and UV radiation. Accordingly, this study focused on the Structural Sealant Glazing (SSG) method. As continuous glazing beads along the glass edges are not required, timber exposure to the exterior can be avoided. This isolates the timber from weathering factors such as wind, rain, and UV radiation, thereby enabling the realization of long-life wooden sashes. It should be noted that mechanical retaining devices are required under national regulations in some European countries—for example, in Germany, according to DIBt approval practice, for installations exceeding a height of 8 m, and in France, under the CSTB framework, regardless of installation height. Furthermore, the timber SSG method offers several advantages, listed below, reducing environmental impact while maintaining design flexibility.

- By eliminating aluminum and using timber exclusively, the system achieves higher thermal insulation performance than conventional SSG. This is expected to prevent and reduce HVAC loads (heating, ventilation, and air conditioning). It should be noted that wooden mullions have been reported to exhibit lower condensation resistance compared to aluminum mullions. Therefore, careful detailing—such as improving insulation at IGU spacers and bolts and introducing a well-defined thermal break—is necessary.
- While aluminum is recyclable, its production process is highly energy intensive. In contrast, timber requires only basic machining (such as cutting and milling), which reduces energy consumption and CO_2 emissions during the manufacturing phase. In addition, carbon storage during growth, together with credits obtained through energy recovery (incineration) and reuse at the end-of-life stage, results in a negative value over the entire life cycle, demonstrating a high environmental advantage.
- The use of aluminum profiles requires expensive extrusion dies and involves difficult bending processes, leading to higher costs and longer lead times. By utilizing timber, complex geometries and free-form designs can be produced easily and cost-effectively through CNC machining.

2. Background of the Study

Structural Sealant Glazing (SSG) has evolved since the 1960s primarily as a bonding material between glass and metal (aluminium) substrates. Feldmann and Kasper et al. (2014) summarised a theoretical and experimental framework for utilizing SSG as a structural material, organizing an evaluation system centered on H-piece tensile testing based on ETAG 002 (now EAD 090010-00-0404) and ASTM C1135. While these early studies were predicated on metal substrates and did not initially assume timber applications, research into wood began around 2000, spurred by the growing trend toward sustainable and resource-efficient architecture. Currently, the ift-guideline VE-08/4 (2017), developed by ift Rosenheim since the late 2000s, serves as the standard evaluation method for timber applications and defines specific ageing scenarios tailored to wooden substrates. Recent research has revealed that timber substrates present unique challenges not encountered with metal substrates, such as aluminium, leading to a wealth of new technical insights. Furthermore, studies are increasingly addressing practical design, indicating that research is progressing from small-scale element testing toward a full-scale testing phase aimed at real-world implementation. Moreover, in recent years, increasing attention has been paid to the environmental aspects of using timber.

- Serrano (2000) demonstrated that machining (such as cutting) of the wood surface can result in loose wood fibres that act as mechanically weak sections, called a mechanically weak boundary layer (MWBL) on the wood surface. He showed that the presence of this layer can lead to a reduction in the strength of adhesive-bonded joints.
- Blyberg (2011) demonstrated that it is essential to address the stresses imposed on the adhesive interface by the moisture-induced deformations (swelling and shrinkage) of timber. She showed that silicone, owing to its low stiffness, provides high deformation capacity, allowing it to deform along with the wood, and excels in its load distribution ability.
- Pantaleo et al. (2012) demonstrated the influence of wood species (such as Meranti, White Oak, and Pine) on tensile adhesion strength. In particular, Pine showed a higher tendency for Adhesive Failure (AF), which is considered to be influenced by resin components in the wood. They showed that the primer treatment produces a "flattening effect" (flats the differences). This treatment minimizes the performance variations among different species and improves overall adhesion performance.
- Pantaleo et al. (2013) conducted tensile and shear tests and revealed that the measured stiffness was only about 50% of the values reported by the manufacturer. In addition, finite element analyses were performed, demonstrating that material properties based on a Rayleigh distribution provide more accurate evaluations than conventional linear models. Furthermore, they pointed out an "edge effect" where increasing the sealant thickness leads to higher shear forces at the edges due to the Poisson effect (cross-sectional deformation). They also noted that the reduction in the central cross-sectional area during loading causes an increase in tensile stress within the sealant.
- Pantaleo et al. (2014) proposed a novel wooden window frame typology from a practical perspective, considering maintainability through a design that allows for the easy disassembly and substitution of glass. This innovation involves applying structural silicone sealant only to a single glass layer of the double-glazing unit, which reduces material quantity and facilitates repairs. Furthermore, they conducted the experimental validation of a finite element (FE) model to ensure that this manufacturing approach maintains acceptable frame stiffness under external loads.
- Nicklisch et al. (2014) categorized 11 commercially available adhesives into three groups based on their stiffness (low, intermediate, and high stiffness) and conducted tests under varying temperatures (-20°C to +80°C) and different load rates (1, 5, and 50 mm/min). The results demonstrated a clear dependency where higher load rates and lower temperatures led to an increase in both strength and stiffness. Furthermore, they classified the failure modes by adhesive type, observing that stiff epoxies exhibited ductile behaviour after reaching a maximum load, while silicones (soft adhesives) showed an approximately linear stress-strain relationship.
- Nicklisch et al. (2016a) conducted accelerated ageing tests based on the four scenarios defined in the ift-guideline VE-08/2—comprising UV exposure, immersion in cleaning solution, changes in moisture content (wetting/drying), and exposure to a SO_2 atmosphere. They clarified that silicone, characterized by its low stiffness and high weathering resistance, exhibits excellent stability under these conditions. Furthermore, they referred to practical design examples, such as the timber-glass composite façade system developed by UNIGLAS.
- Nicklisch et al. (2016b) evaluated combinations of seven timber substrates—comprising solid softwoods and hardwoods (pine, larch, beech, and oak), LVL (laminated beech veneer lumber), densified laminated wood, and chemically modified wood—with a silicone adhesive. They concluded that durability strongly depends on the chosen wood species, noting that only solid pine and beech were able to maintain residual strength within the permissible range after immersion degradation. They pointed out that the examined laminated and densified materials are unsuitable for such conditions, as the moisture expansion (swelling) of the wood itself during immersion causes the joint

to self-destruct (premature failure) before testing. For difficult-to-bond species such as oak, they demonstrated that adhesion performance could be significantly improved through re-planing immediately before bonding or by applying specific primers. Furthermore, scanning electron microscope (SEM) observations verified that planing reduces "loose particles" on the wood surface, while the primer smoothes the surface and aids penetration into the wood cells, thereby enabling the achievement of nearly 100% cohesive failure within the sealant.

- Fadai et al. (2020) demonstrated that substituting the conventional aluminum support structure of a façade with timber materials (such as glulam or LVL) can reduce the non-renewable primary energy demand during the manufacturing phase (Cradle-to-gate) by approximately 86.7%, decreasing from 1,043.37 MJ/m² to just 138.97 MJ/m². Regarding Global Warming Potential (GWP), while the manufacturing of aluminum-glass façades results in emissions of 74.97 kg CO_2 equivalent, timber-based systems record a negative value of -0.72 kg CO_2 equivalent. This is due to the carbon storage effect during the growth of the wood, which allows the building component to function as a carbon sink. In the End-of-Life (EoL) phase, aluminum offers a credit of -57.70 kg CO_2 equivalent, as its recycling can recover about 76% of the non-renewable primary energy released during production. Conversely, timber components contribute an EoL credit of -13.92 kg CO_2 equivalent through energy recovery (incineration) and potential reuse or recycling into wood-based materials. Ultimately, while aluminum exhibits higher recovery efficiency through recycling, the timber system maintains an extremely high environmental advantage over its entire life cycle by combining its inherently low manufacturing footprint with its unique capacity for long-term carbon sequestration.
- Choquet (2023) conducted thermal simulations and demonstrated that timber mullions are significantly superior in thermal insulation performance, with U-values averaging 59% lower than those of aluminum mullions. This performance improvement translates to a 14% lower average U-value for the overall curtain wall and a 7% reduction in the whole-building Thermal Energy Demand Intensity (TEDI). Conversely, the study confirmed that timber systems are inferior in condensation resistance (CR), with values averaging 12% lower than their aluminum counterparts. While the high conductivity of aluminum results in a uniform temperature distribution, timber's high thermal resistance causes heat flow to concentrate at the remaining metallic components, such as bolts and IGU spacers. These components act as thermal bridges where interior surface temperatures drop sharply, thereby creating a localized risk of condensation. The research confirmed that this risk can be mitigated by improving the insulation performance of the IGU and its spacers, and emphasized the critical importance of incorporating a clear thermal break, particularly at mechanical fasteners.
- Nguyen et al. (2026) quantitatively demonstrated that the thermal performance of curtain wall frames can be dramatically improved by adopting a composite design where aluminum mullions, which possess a very high thermal conductivity of approximately 160 W/m·K, are encased in low-conductivity timber such as cedar (0.094 W/m·K) or pine (0.14 W/m·K). This configuration effectively interrupts the thermal bridges that serve as the primary heat flow paths. The study confirmed that for captive glazing systems (Type 1), the composite design reduced the U-value from 12.31 W/m²·K to 5.21 W/m²·K (approximately a 58% reduction), while structural glazing systems (Type 2) achieved a significant reduction of approximately 55%, decreasing from 7.05 W/m²·K to 3.21 W/m²·K.

Turning to trends in Japan, the Structural Sealant Glazing (SSG) method was widely adopted from the 1980s through the early 1990s. However, its use declined in the late 1990s due to concerns regarding adhesive reliability. In 2003, SSG was first incorporated into JASS 17 as a formal standard; however, its scope was limited mainly to two-edge structural glazing systems. Meanwhile, in the United States, Europe, and other parts of Asia, technical guidelines have been established, and the method is

currently in widespread use. The first editions of ASTM C1401, ETAG 002, and JGJ 102 were published in 1998, 1999, and 2003, respectively. In Japan, there has been a renewed movement to popularize the SSG method, driven by increasing interest in its advantages, such as design flexibility and thermal performance. Following a series of research studies by Matsuo et al. (2013–2025), the Japan Sealant Industry Association (JSIA) published "JSIA 005:2025: Standard test methods of sealants for structural glazing in buildings" in 2025, establishing a standardized Japanese framework for testing. Table 1 introduces the test items and required performance values. For the purpose of this study, the symbol X is defined to represent the mean maximum tensile stress, and RX is defined as the residual strength ratio relative to the reference value at 23°C. Also, the symbols s and $R_{u,5}$ represent the standard deviation and the characteristic breaking stress, respectively, according to ETAG 002 (now EAD 090010-00-0404).

However, the adherends (substrates) remain limited primarily to aluminium, and research regarding adhesion to timber has not yet been fully conducted. In this study, verification tests were performed by substituting the substrate with timber, with the objective of satisfying all required performance values. During the testing process, challenges unique to timber were encountered—including the influence of wood species, surface treatment, primer type, fiber direction (grain orientation), wood extractives, and the selection of weather-resistant coatings. Despite these factors, specifications that fulfil all performance requirements were successfully established. For this research, SEALANT-FC-295SG (Shin-Etsu Chemical Co., Ltd.) was utilized. Given that this product has already satisfied the criteria in glass-to-aluminium evaluations, this study excludes tests for tear durability (notched tensile testing), workability, and curing properties, which are intended to verify the performance of the sealant material itself. Instead, performance verification tests were conducted only for the following items specifically related to wood surface adhesion. The loading rate (crosshead speed) was set to 50 mm/min, which is close to 50.8 ± 5.1 mm/min, in accordance with ASTM C1135-19.

Conditioning before tensile test

a. Tensile Adhesion Test after Curing (Initial Mechanical Strength)
   Specimens were subjected to “A-curing” for 28 days under conditions of 23 °C and 50 % RH. This curing was performed before the subsequent conditioning.
b. Tensile Adhesion Test after Cyclic shear loading (Durability)
   A new durability category, "9030SG," was established by increasing the number of cycles in the cyclic fatigue test from 2,000 to 20,000 cycles, based on the 9030G conditions specified in JIS A 1439 (30% shear deformation in both directions).
c. Tensile Adhesion Test after Hot Water Immersion (Water Resistance)
   Specimens were immersed in hot water at 50°C for 7 days. Upon removal, the specimens were conditioned (allowed to rest) at 23°C and 50% RH for 24 ± 4 hours.
d. Tensile Adhesion Test after Artificial Light Exposure (Weathering Resistance)
   1,000 hours of exposure to an open-flame carbon arc lamp with water spray (Symbol WS-A as specified in Table 1 of JIS A 1415), or 1,300 hours of exposure to a xenon-arc lamp with water spray (Exposure cycle No. 2 or No. 10 of Method A, as specified in 4.1.1 of JIS K 7350-2).

Table 1: Structural sealant performance according to JSIA 005.

Type	Condition	adherend	Number of specimens	Temperature during the test	Average tensile stress	Criteria
Initial mechanical strength (Chapter 4)	Standard cure of the sealant	Glass Aluminum	10	23℃	X_{23} (Reference Value)	$X_{23} \geqq 0.84 N/mm^2$ CF≧90%
		Glass Aluminum	5	-20℃	X_{-20}	$RX_{-20}=X_{-20}/X_{23} \geqq 0.7$ $X_{-20} \geqq 0.70 N/mm^2$ CF≧90%
		Glass Aluminum	5	80℃	X_{80}	$RX_{80}=X_{80}/X_{23} \geqq 0.7$ $X_{80} \geqq 0.70 N/mm^2$ CF≧90%
Residual strength after ageing (Chapter 5)	Immersion in hot water	Glass Aluminum	3	23℃	X_{HW}	$RX_{HW}=X_{HW}/X_{23} \geqq 0.7$ $X_{HW} \geqq 0.70 N/mm^2$ CF≧90%
	Artificial light exposure	Glass	3	23℃	X_{UV}	$RX_{UV}=X_{UV}/X_{23} \geqq 0.7$ $X_{UV} \geqq 0.70 N/mm^2$ CF≧90%
	Cyclic shear loading	Aluminum	3	23℃	X_{CL}	$RX_{CL}=X_{CL}/X_{23} \geqq 0.7$ $X_{CL} \geqq 0.70 N/mm^2$ CF≧90%
	Resistance to tearing	Glass	3	23℃	X_{RT}	$X_{RT}/X_{23} \geqq 0.7$ $X_{RT} \geqq 0.70 N/mm^2$ CF≧90%
Workability Curability (Chapter 6)	elastic recovery test	-	3	23℃	-	≧95%
	volume loss test	-	3	-	-	≦10%

3. Specification study of timber SSG sealants

3.1. Screening tests for selecting appropriate timber species

In this study, first, as illustrated in Fig. 1, we screened for desirable wood specifications by conducting H-piece tensile tests and S-piece shear tests on various timber configurations. To minimize variability, standardized lumber with a moisture content (MC) of 15% or less was used. The structural silicone sealant employed was SEALANT-FC-295SG (Shin-Etsu Chemical Co., Ltd.); X-33-270 primer was used for S-type shear specimens, and X-33-270-2 was used for H-piece tensile specimens. The loading rate (crosshead speed) was set to 50 mm/min in accordance with JSIA 005. Tests were performed in the initial state and after immersion degradation. While the hot water immersion condition specified in JSIA 005 is 50°C, tests were initially conducted at a milder temperature of 23°C to assess the baseline aging behavior. Regarding wood surface treatment, preliminary tests indicated that sanding caused

wood failure (substrate failure) due to the roughened surface irregularities (Fig. 2). Since no significant difference in performance was observed between planing and super-planing (ultra-precision planing), planing was adopted for its ease of production. The failure in sanded specimens is attributed to the formation of a mechanically weak boundary layer (MWBL) on the timber surface, as identified by Serrano (2000) and Nicklisch et al. (2016b).

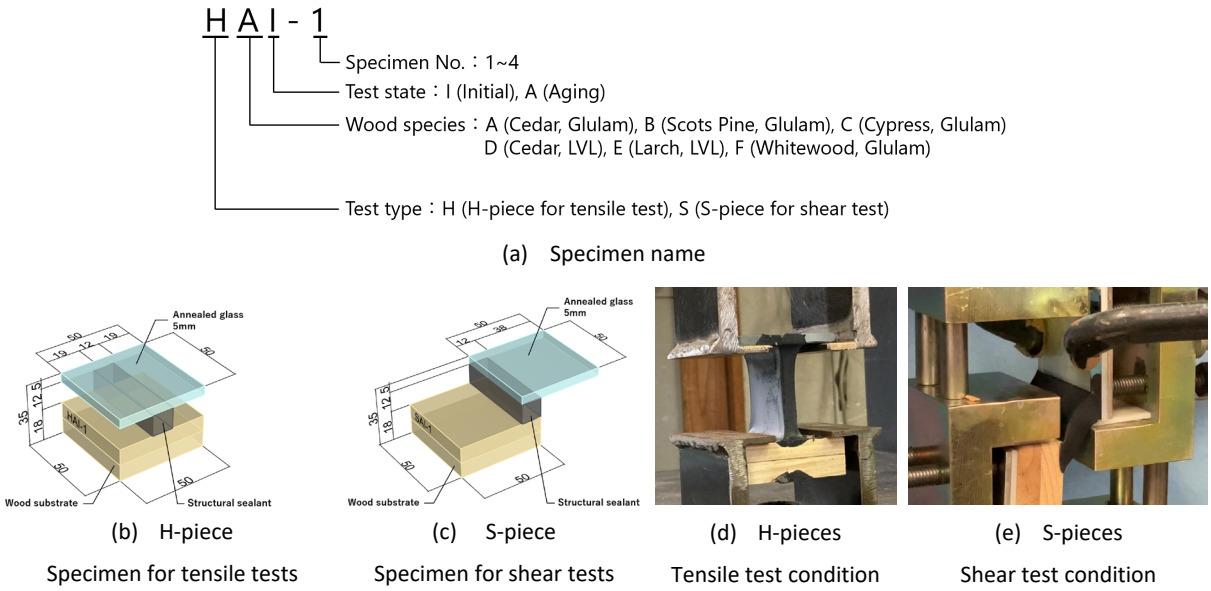

Fig. 1: Outline of the test.

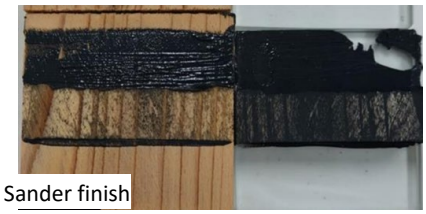

Fig. 2: Condition of the specimen with sander finish after testing.

Tables 2 and 3 present the test results for each timber specification. Red text indicates that the values do not satisfy the required performance values. X_{23}, X_{HW} and RX_{HW} correspond to the parameters defined in Table 1 and represent the mean values of the specimens. All failure mode data represent the values obtained from the specimen exhibiting the minimum percentage of cohesive failure (CF). Regarding the failure modes: CF denotes cohesive failure within the sealant, tCF denotes thin-layer cohesive failure (near-surface cohesive failure) within the sealant, AF denotes adhesive failure at the timber interface, MF denotes material failure (substrate failure) of the timber.

- Wood species A achieved good adhesion in its initial state; however, it exhibited adhesive failure (AF) at the timber surface after immersion (Fig. 3: HAA-4). No cases of wood failure (MF) were observed.
- Similar to species A, wood species B showed adhesive failure (AF) after immersion (Fig. 3: HBA-4). In the S-piece shear test after immersion, there was one instance (SBA-1) where wood failure (MF) occurred before the sealant reached its breaking point.
- Wood species C demonstrated good initial adhesion, but many instances of thin-layer cohesive failure (tCF) (near-surface cohesive failure) were observed after immersion (Fig. 3: HCA-2). In

specimens HCA-1 and SCA-4 after immersion, wood failure (MF) was identified, where the timber peeled along the fiber direction.

- Wood species D and E are LVL (laminated veneer lumber) consisting of laminated thin veneers. These frequently exhibited MF, where the first veneer layer of the bonding surface peeled off before the sealant failed (Fig. 3: HDI-4, HEI-4). This resulted in insufficient wood strength to support the joint.
- Wood species F is a soft whitewood glulam (glued laminated timber) which frequently showed wood failure (MF) before sealant failure (Fig. 3: HFI-4). Consequently, the wood strength was found to be insufficient.

Based on these results, wood species D, E, and F are considered unsuitable as adherends because wood failure (substrate failure) was the dominant failure mode. This is consistent with the report by Nicklisch et al. (2016b). While species A and B frequently exhibited adhesive failure (AF), wood species C showed a high proportion of thin-layer cohesive failure (tCF) (near-surface cohesive failure) in the tensile tests after immersion, indicating relatively better adhesion. Therefore, wood species C was adopted for the subsequent tests. Fig. 4 shows the stress-strain curves for the cypress glulam (glued laminated timber) specimens (Species C). In the H-piece tensile tests, degradation was observed after hot water immersion, as evidenced by a decrease in both strength and stiffness. The mean maximum tensile stress (X_{HW}) slightly exceeded the required performance value of 0.7 N/mm². However, the residual strength ratio (RX_{HW}) was 53%, which fell below the criteria of 70%. In contrast, the S-piece shear tests demonstrated a high residual strength ratio (RX_{HW}) of 89.5%, showing almost no reduction in strength despite a decrease in stiffness.

Table 2: Results of tensile tests of H-pieces.

	unit	Standard cure of the sealant（23℃）						Immersion in hot water（23℃）					
		A	B	C	D	E	F	A	B	C	D	E	F
X_{23}, X_{HW}	N/mm²	1.22	1.33	1.32	0.63	0.92	1.19	0.64	0.38	0.70	0.51	0.3	0.45
RX_{HW}	%	-	-	-	-	-	-	52.5	28.6	53.0	81.0	32.6	37.8
CF	%	95	100	100	0	0	15	0	0	0	0	0	0
tCF	%	5	0	0	0	0	0	0	0	80	0	0	0
AF	%	0	0	0	0	0	0	100	100	0	0	100	75
MF	%	0	0	0	100	100	85	0	0	20	100	0	25

Table 3: Results of shear tests of S-pieces.

	unit	Standard cure of the sealant（23℃）						Immersion in hot water（23℃）					
		A	B	C	D	E	F	A	B	C	D	E	F
X_{23}, X_{HW}	N/mm²	1.12	1.11	1.05	0.84	0.74	0.95	0.94	1.02	0.94	0.70	0.33	0.75
RX_{HW}	%	-	-	-	-	-	-	83.9	91.9	89.5	83.3	44.6	78.9
CF	%	100	100	100	0	0	99	95	0	80	0	0	0
tCF	%	0	0	0	0	0	0	0	0	0	0	0	0
AF	%	0	0	0	0	0	0	5	0	0	0	0	0
MF	%	0	0	0	100	100	1	0	100	20	100	100	100

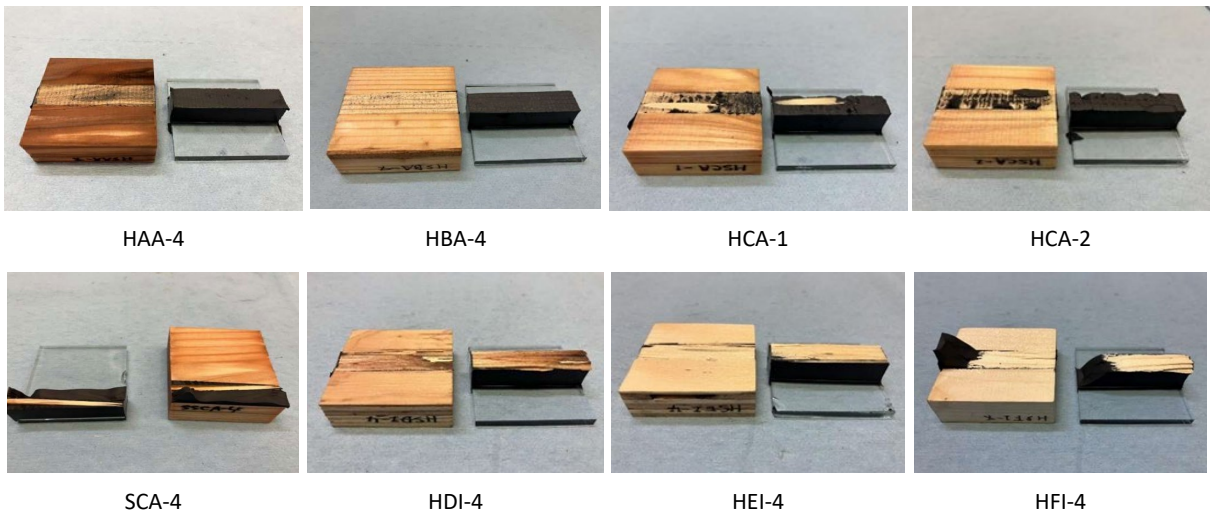

Fig. 3: Conditions of the specimens after testing.

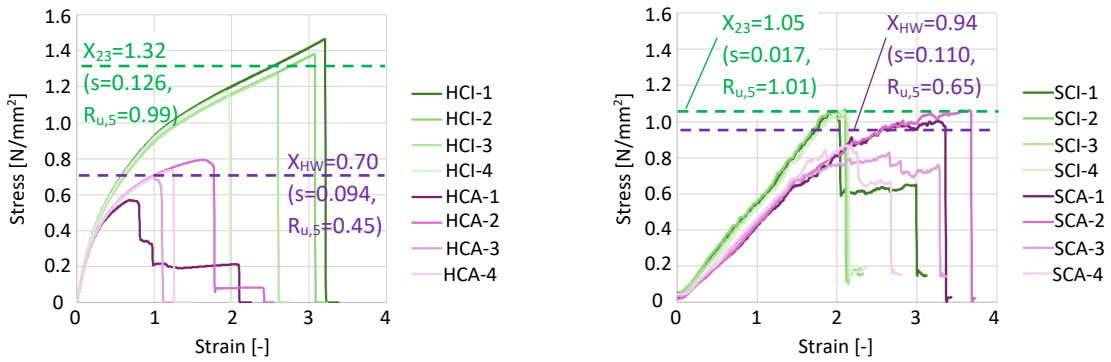

(a) H-pieces, tensile test (b) S-pieces, shear test

Fig. 4: Stress-strain curve (C: Cypress, Glulam).

3.2. Primer improvement for enhanced adhesion performance after immersion in hot water

The screening tests described above successfully identified potential timber species. However, even with the selected Cypress glulam (Species C), tensile tests after immersion resulted in thin-layer cohesive failure (tCF) (near-surface cohesive failure), indicating that satisfactory adhesion had not yet been achieved. Consequently, additional tests were conducted using improved primers, specifically X-33-270-3 and X-33-270-4, which feature modified adhesive and film-forming components tailored for wood applications. Cypress glulam continued to be utilized as the timber substrate (adherend). To specifically verify the adhesion to the wood surface, the specimens were designed so that the longitudinal direction of the sealant was perpendicular to the grain direction; this orientation was chosen to minimize the occurrence of the wood failure (MF) along the fibers that had been observed in Section 3.1. The test conditions were implemented in accordance with JSIA 005, as described in Chapter 2. Furthermore, since the results in Section 3.1 indicated that the H-piece tensile test was more effective than the S-piece shear test at representing degradation, only H-piece tensile tests were performed.

As shown in Fig. 5(a), the percentage of cohesive failure (CF) was 100% for both primers, indicating that the thin-layer cohesive failure (tCF) (near-surface cohesive failure) encountered during the screening tests was resolved and satisfactory adhesion was achieved. Fig. 5(b) illustrates the stress-

strain curves. In the tensile tests following hot water immersion at 50°C, the mean maximum tensile stresses (X_{23} and X_{HW}) exceeded the required performance value of 0.7 N/mm². Pantaleo et al. (2012) and Nicklisch et al. (2016b) also emphasize the critical importance of primer treatment for improving adhesion strength to timber substrates. Regarding the residual strength ratio (RX_{HW}) after hot water immersion—referenced against the results of the screening test primer X-33-270-2—the values reached 64% for X-33-270-3 and 76% for X-33-270-4, which are approximately the JSIA 005 required value of 70%. While SEALANT-FC-295SG achieves a residual strength ratio of 80% or higher in glass-to-aluminum configurations, the use of timber as the adherend is considered the factor leading to the reduction in the residual strength ratio during immersion. For reference, other international standards specify a minimum residual strength ratio of 75% in ETAG 002 (now EAD 090010-00-0404) and 50% in ift VE-08/4.

Primer: X-33-270-3 CF=100%

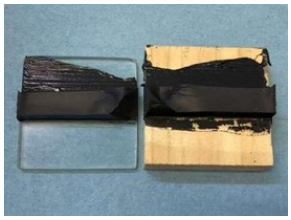

Primer: X-33-270-4 CF=100%

(a) Conditions of the specimens after testing

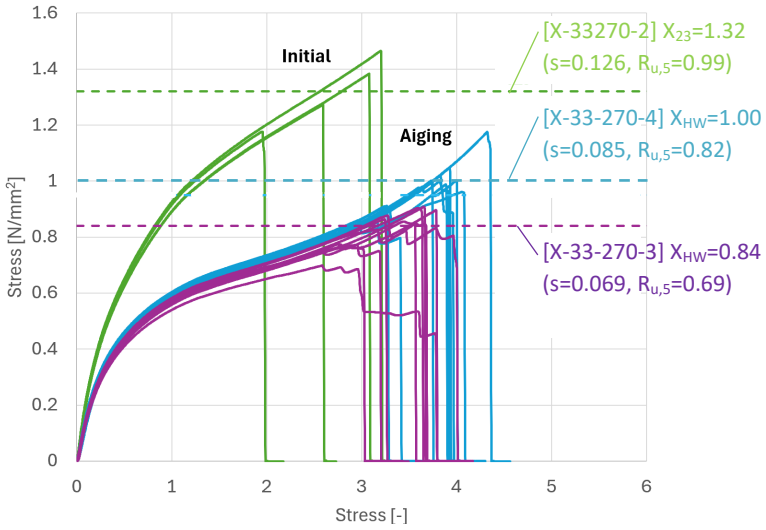

(b) Stress-displacement curve (C: Cypress, Glulam)

Fig. 5: Test Results after Immersion in hot water (50℃).

3.3. Study on the effects of water-leached extractives from timber

In Section 3.2, a phenomenon was observed where the residual strength ratio decreased when timber was used as an adherend, compared to standard glass-to-aluminum specimens. This is considered to be influenced not only by sealant degradation due to hot water immersion but also by wood extractives leaching into the water. As illustrated in Fig. 6(a) and 6(b), glass-to-glass specimens were prepared and immersed both with and without wood pieces enclosed in the plastic bag to verify the differences in the residual strength ratio. To isolate the influence of the wood alone, no primer was applied. Regarding the wood species, Cypress glulam was used along with Red pine lumber, thermally modified Red pine, Larch lumber, and thermally modified larch for comparison. The test conditions were implemented in accordance with JSIA 005.

Table 4 presents the test results. The residual strength ratio (RX_{HW}) after hot water immersion was 89% for specimens without wood, whereas it ranged from 71% to 76% for specimens immersed with wood pieces. These results clarify that even without direct contact between the timber and the sealant, wood extractives cause a reduction in the residual strength ratio during hot water immersion. Particularly with larch, visual defects such as sealant foaming (bubbling) were also observed, as shown in Fig. 6(d).

(a) Specimens and woods (b) Enclosed in a plastic bag (c) Without wood (d) With thermally modified Larch

Fig. 6: Conditions of the specimens before and after testing.

Table 4: Results of tensile tests of H-pieces.

	unit	Standard cure of the sealant (23℃)	Immersion in hot water (50℃)					
			Without wood	Glulam Cypress	Lumber Larch	Thermally modified Larch	Lumber Red pine	Thermally modified Red pine
X_{23}, X_{HW}	N/mm^2	1.16	1.03	0.83	0.84	0.86	0.88	0.87
RX_{HW}	%	-	89	71	72	74	76	75
CF	%	100	100	100	100	100	100	100

In Chapter 3, tests were conducted on six different timber specifications, revealing that adhesion performance and timber strength vary depending on the timber species, and that Cypress glulam is the most suitable. In addition, the use of a primer modified specifically for timber significantly improved adhesion performance, indicating that appropriate primer selection is essential for ensuring long-term reliability. On the other hand, the residual strength ratio obtained from tensile tests was found to be lower than that of conventional aluminium–glass specimens.

To investigate the cause of this reduction in residual strength ratio, immersion tests were conducted in which glass–glass specimens and wood pieces were immersed together in a plastic bag. The results showed that the residual strength ratio decreased even when the SSG sealant was not in direct contact with the timber, and in the case of larch, surface defects such as foaming of the sealant were also observed. These findings indicate that extractives leached from timber into water affect the performance of the sealant.

4. Performance verification tests of timber SSG sealants

In this chapter, a series of test protocols defined in JSIA 005 were conducted on Cypress glulam (glued laminated timber), the specifications for which were selected in the preceding chapters, to verify the adhesion of SSG (Structural Sealant Glazing) to timber. In addition to the X-33-270-3 primer used in the previous chapter, X-33-271 was newly introduced for this stage of the research. X-33-270-4 was not adopted because adhesive failure (AF) was observed in some cases during peel tests performed in a wet state after immersion. Given that X-33-270-4 contains a lower concentration of film-forming and adhesive components compared to X-33-270-3, it is considered that a higher component concentration is more advantageous for adhesion performance following immersion. X-33-271 was developed by improving the adhesive components to maintain adhesion even at a lower concentration, while its viscosity was reduced to improve workability (ease of application). Furthermore, in tensile adhesion

tests after hot water immersion and accelerated weathering (artificial light exposure), experiments were conducted with the application of weather-resistant coatings to investigate their effectiveness.

4.1. Tensile test after standard cure of the sealant （Initial mechanical strength）

Following A-curing (28 days under conditions of 23°C and 50% RH), H-piece tensile tests were conducted at environmental temperatures of 23°C, -20°C, and 80°C. The resulting stress-strain curves are illustrated in Figs. 7, 8, and 9. Under all primer conditions, the percentage of cohesive failure (CF) was 100%, and the mean maximum tensile stresses (X_{23}, X_{-20}, X_{80}) as well as the residual strength ratios (RX_{-20}, RX_{80}) exceeded the required performance values specified in Table 1.

As noted by Nicklisch et al. (2014), the maximum tensile stress typically increases as temperature decreases and decreases as temperature increases. In the specific cases of specimens X-33-271-4 and X-33-271-5 at -20°C, glass failure occurred before the sealant reached cohesive failure. The mean maximum tensile stress at 23°C (X_{23}) serves as the reference value for calculating the residual strength ratio (RX) in other tests following degradation.

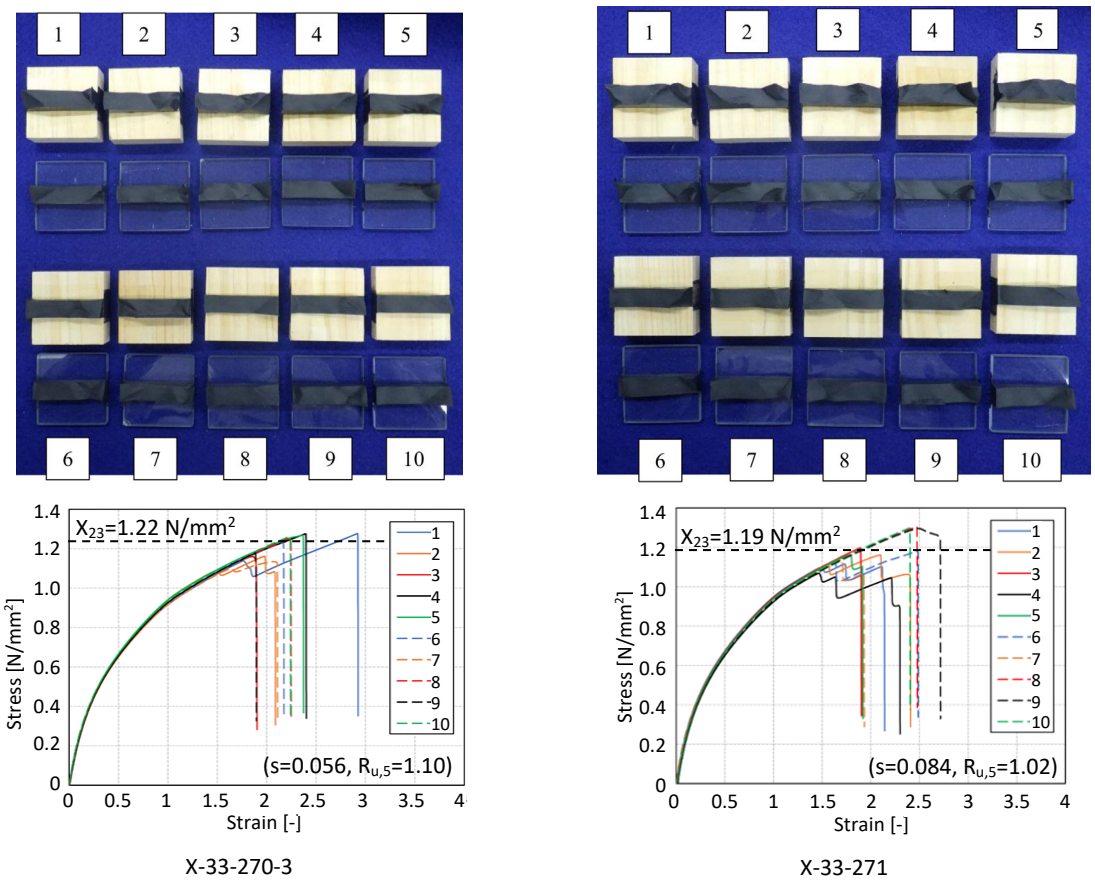

Fig. 7: Stress-strain curve (Initial mechanical strength, 23℃).

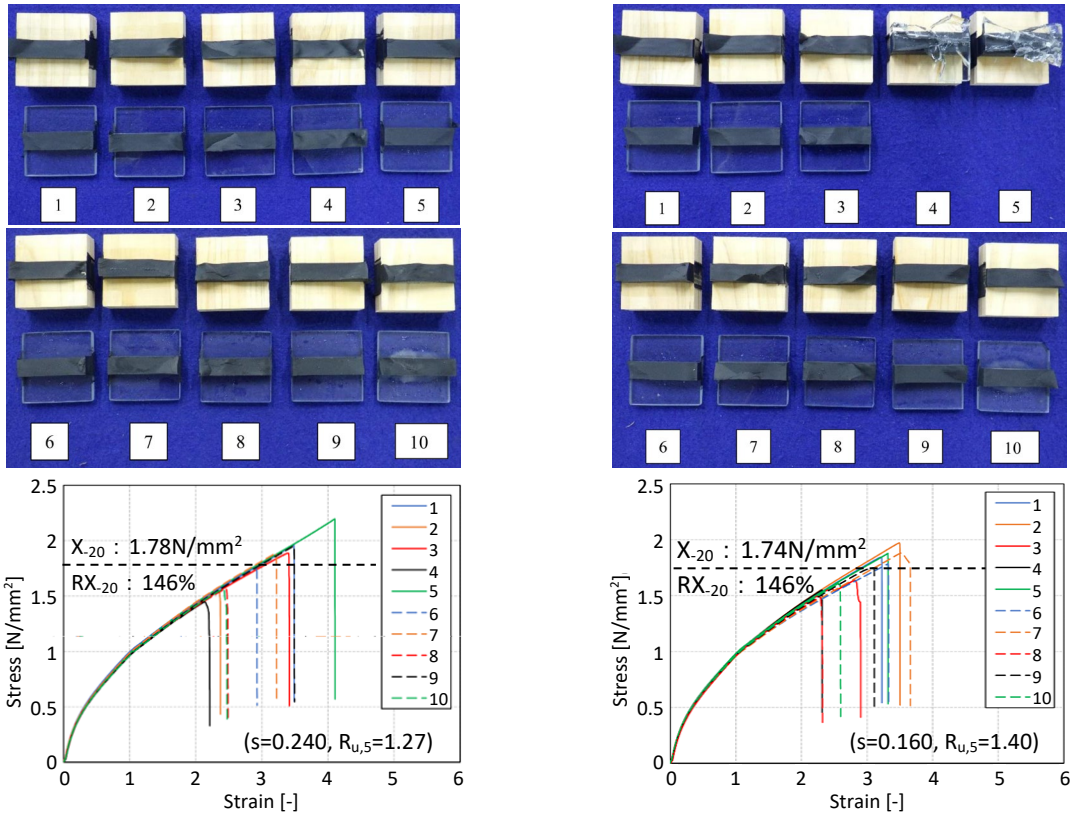

Fig. 8: Stress-strain curve (Initial mechanical strength, -20℃).

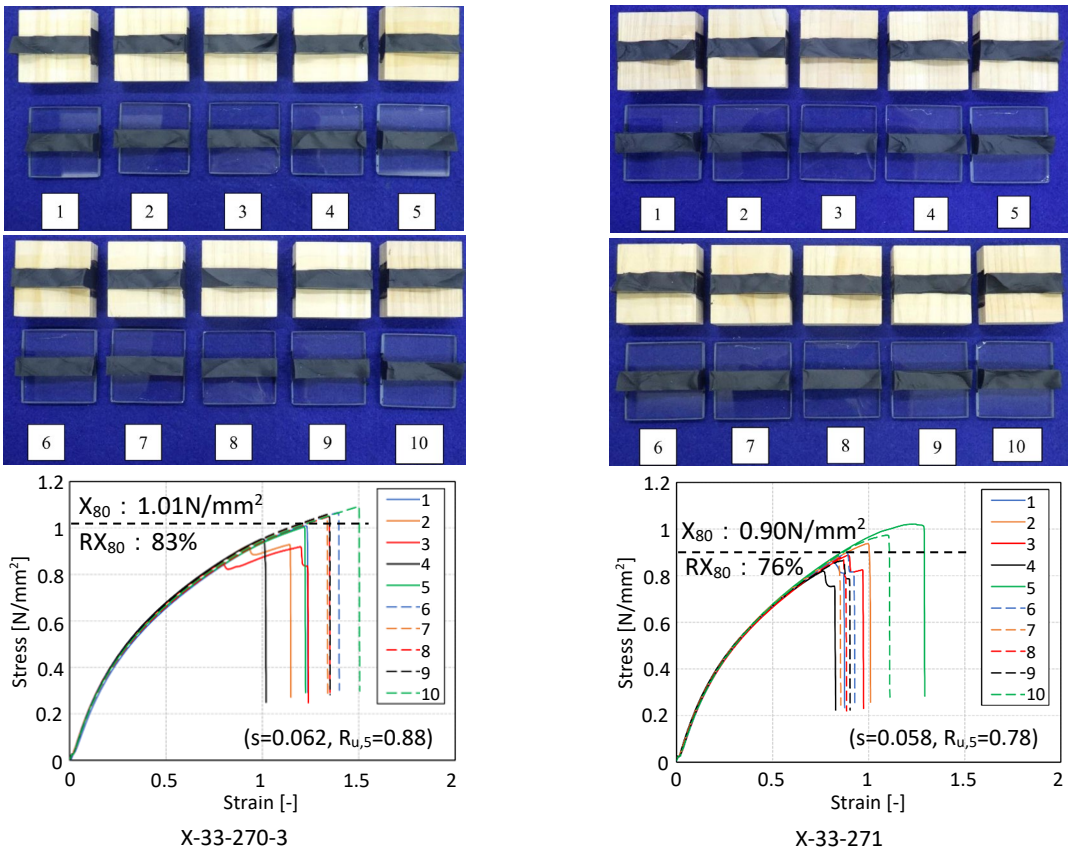

Fig. 9: Stress-strain curve (Initial mechanical strength, 80℃).

4.2. Tensile test after Cyclic shear loading (Residual strength after ageing)

H-piece tensile tests were conducted following the durability test specified in JSIA 005, which involves applying 20,000 cycles of ±30% shear deformation repeatedly in the longitudinal direction of the sealant. Fig. 10 illustrates the resulting stress-strain curves. Under all primer conditions, the percentage of cohesive failure (CF) was 100%, and both the mean maximum tensile stress (X_{CL}) and the residual strength ratio (RX_{CL}) exceeded the required performance values specified in Table 1. Compared to the 23°C reference test results in Section 4.1, the specimens exhibited lower stiffness and higher elongation at break.

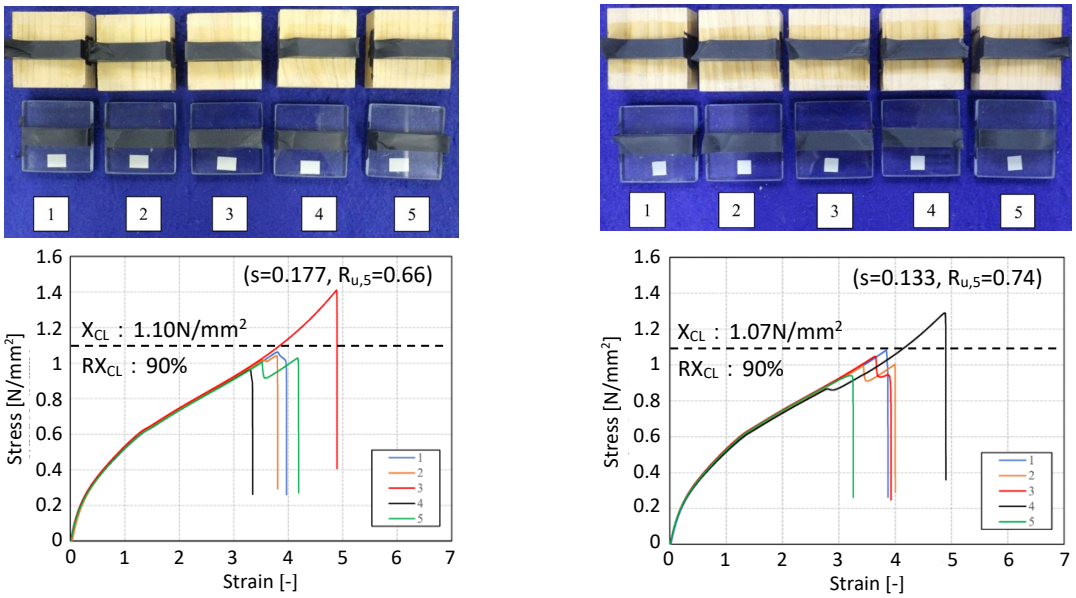

Fig. 10: Stress-strain curve (Cyclic shear loading).

4.3. Tensile test after Immersion in hot water (Residual strength after ageing)

Tensile adhesion tests were conducted after hot water immersion. Since Section 3.2 clarified that wood extractives leaching during hot water immersion reduce the residual strength ratio (RX_{HW}), it was verified whether weather-resistant coatings also exert any negative impact. Eight types of weather-resistant coatings were utilized, as shown in Table 5. All of these were one-component systems and were selected as transparent coatings to preserve the appearance of the wood grain. The number of specimens was set to two for each test configuration.

The weather-resistant coatings were applied using two methods: pre-application (before sealant application) and post-application (after sealant application).Table 6 presents the specimen combinations and test results, and Fig. 11 illustrates the post-test condition. Cases where the residual strength fell below the criteria (RX_{HW}<70%) shown in Table1 are indicated with a triangle (△). For reference, the pre-application procedure is specified in ift VE-08/4.

Table 5: Type of weather-resistant coating.

a	Semi-film-forming	Inorganic (borate)	Water-based	flame retardancy・resistance to decay, insects, and Mold・antibacterial property
b	Penetrating	Organic (alkyd)	Oil-based	UV protection, water repellence, and resistance to decay, insects, and Mold
c	Semi-film-forming	Organic (alkyd)	Oil-based	moisture permeability・UV protection・resistance to weather, decay and Mold
d	Film-forming	Organic (acrylic)	Water-based	waterproofness・resistance to wear, slip and chlorine
e	Film-forming	Organic (silicone)	Water-based	water repellence、weather resistance、low VOC、metal-catalyst-free
f	Penetrating	Organic (silicone)	Oil-based	water repellence、waterproofness、resistance to weather, Mold and algae resistance、low VOC
g	Film-forming	Organic (CNF + urethane)	Water-based	UV protection・discoloration prevention protective coating・high durability
h	Film-forming	Organic (CNF)	Water-based	UV protection・discoloration prevention protective coating・high durability

In the pre-application series, coatings d, e, g, and h, which utilized film-forming coatings, exhibited adhesive failure (AF) at the interface following immersion. In particular, coating e, which forms a water-repellent film, repelled the primer, making consistent primer application difficult. While semi-film-forming coatings a and c exhibited some tackiness on the sealant surface, they demonstrated satisfactory adhesion when used in combination with no primer or the X-33-271 primer. Regarding the penetrating-type coatings, coating b achieved 100% cohesive failure (CF) across all primer conditions, indicating excellent adhesion. Coating f also exhibited good adhesion when used with the X-33-270-3 primer. For specimens with CF > 90%, the residual strength ratio (RX_{HW}) ranged from 60% to 76%.

In the post-application series, all combinations of primers and coatings achieved 100% cohesive failure (CF), demonstrating satisfactory adhesion. The residual strength ratio (RX_{HW}) for specimens with CF > 90% ranged from 59% to 71%.

In specimens with CF > 90%, the residual strength ratio (RX_{HW}) remained around the JSIA 005 required performance value of 70%, which is comparable to the results observed in Section 3.2, even when weather-resistant coatings were applied. These results clarify that, provided an appropriate combination is selected, weather-resistant coatings do not exert a negative impact on the tensile adhesion performance. Furthermore, no visual defects or discolorations were observed in the weather-resistant coatings due to wood extractives.

Table 6: Results of tensile tests of H-pieces (Immersion in hot water 50℃).

Type of Coating		Pre-application			Post-application	
		No-primer	X-33-270-3	X-33-271	X-33-270-3	X-33-271
Semi-film -forming	a	△ CF100%/RX_{HW}67%	× CF70%/RX_{HW}59%	△ CF100%/RX_{HW}67%	△ CF100%/RX_{HW}65%	△ CF100%/RX_{HW}67%
Penetrating	b	△ CF98%/RX_{HW}63%	○ CF100%/RX_{HW}76%	△ CF100%/RX_{HW}60%	△ CF100%/RX_{HW}61%	○ CF100%/RX_{HW}70%
Semi-film -forming	c	△ CF98%/RX_{HW}64%	× CF50%/RX_{HW}65%	△ CF100%/RX_{HW}65%	△ CF100%/RX_{HW}68%	△ CF100%/RX_{HW}61%
Film -forming	d	× CF10%/RX_{HW}33%	× CF40%/RX_{HW}49%	× CF30%/RX_{HW}29%	△ CF100%/RX_{HW}60%	△ CF100%/RX_{HW}67%
Film -forming	e	△ CF97%/RX_{HW}68%	× CF15%/RX_{HW}69%	× CF85%/RX_{HW}71%	△ CF100%/RX_{HW}60%	△ CF100%/RX_{HW}61%
Penetrating	f	× CF0%/RX_{HW}56%	△ CF100%/RX_{HW}67%	× CF0%/RX_{HW}73%	△ CF100%/RX_{HW}59%	△ CF100%/RX_{HW}68%
Film -forming	g	△ CF98%/RX_{HW}60%	× CF0%/RX_{HW}52%	× CF0%/RX_{HW}13%	△ CF100%/RX_{HW}64%	△ CF100%/RX_{HW}56%
Film -forming	h	× CF40%/RX_{HW}40%	× CF75%/RX_{HW}50%	× CF0%/RX_{HW}32%	△ CF100%/RX_{HW}64%	○ CF100%/RX_{HW}71%

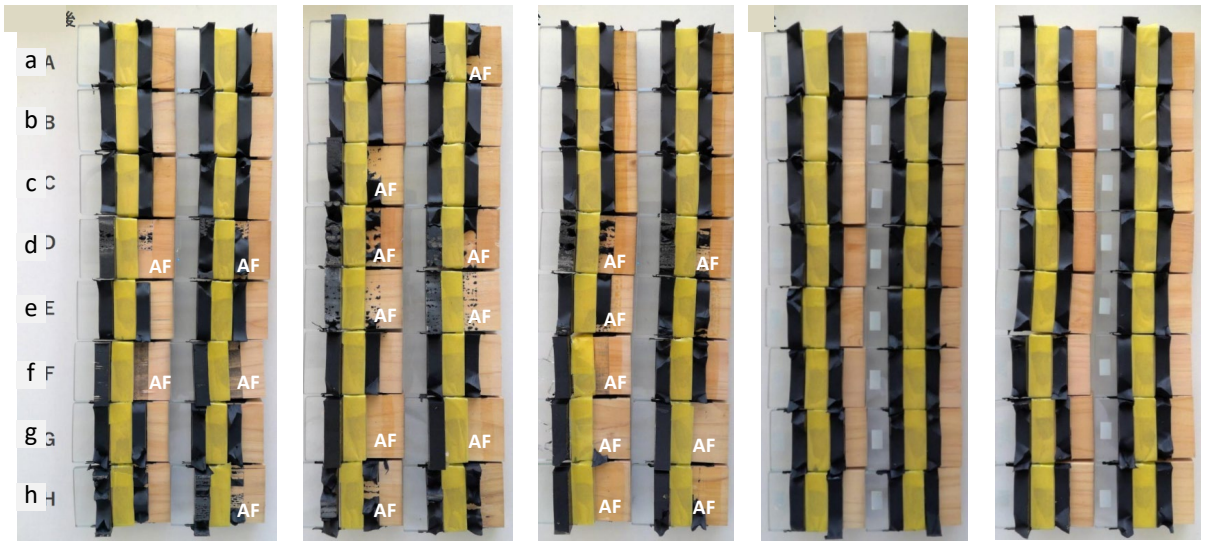

Fig. 11: Conditions of the specimens after testing (Immersion in hot water 50℃).

4.4. Tensile test after Artificial light exposure (Residual strength after ageing)

Tensile adhesion tests were conducted after artificial light exposure. The light source used was sunshine carbon arc, and after 1,000 hours of irradiation, the degradation state of the timber surface

was also examined. The same eight types of weather-resistant coatings as in Section 4.3 were used, with two specimens prepared for each configuration. The specimen combinations and test results are presented in Table 7, and the post-test conditions are illustrated in Fig. 12. Cases where the residual strength fell below the criteria (RX_{HW}<70%) shown in Table1 are indicated with a triangle (△).

In the pre-application series, adhesive failure (AF) occurred at the interface between the coating and the primer for the film-forming coatings (d, e, g, and h). In particular, coating e, which forms a water-repellent film, repelled the primer, making consistent application difficult. Conversely, the penetrating coatings (b and f) and semi-film-forming coatings (a and c) exhibited satisfactory adhesion under all primer conditions; however, coatings a and c showed some tackiness on the sealant surface. For specimens with CF > 90%, the residual strength ratio (RX_{UV}) ranged from 75% to 102%.

In the post-application series, when primer X-33-271 was utilized, adhesive failure (AF) was observed between the coating and the primer for film-forming coatings e, g, and h, as well as semi-film-forming coating a. Other combinations demonstrated good adhesion. The residual strength ratio (RX_{UV}) for specimens with CF > 90% was between 82% and 99%.

Regarding timber surface degradation after artificial light exposure, as shown in Fig. 13, whitening (discoloration) was observed on parts of the irradiated surface for timber treated with coatings b, c, and e, and across the entire irradiated surface for coating f. The order of degradation severity was f > e > b > c. On the other hand, timber treated with coatings a, d, g, and h showed almost no visible changes from their initial state. These results indicate that even with transparent finishes, applying an appropriate weather-resistant coating can effectively mitigate degradation caused by artificial light exposure.

Table 7: Results of tensile tests of H-pieces (Artificial light exposure).

Type of Coating		Pre-application			Post-application	
		No-primer	X-33-270-3	X-33-271	X-33-270-3	X-33-271
Semi-film -forming	a	○ CF100%/RX_{UV}83%	○ CF95%/RX_{UV}78%	○ CF100%/RX_{UV}88%	○ CF100%/RX_{UV}82%	× CF85%/RX_{UV}71%
Penetrating	b	○ CF100%/RX_{UV}85%	○ CF100%/RX_{UV}92%	○ CF100%/RX_{UV}87%	○ CF100%/RX_{UV}91%	○ CF100%/RX_{UV}82%
Semi-film -forming	c	○ CF100%/RX_{UV}80%	○ CF100%/RX_{UV}98%	○ CF100%/RX_{UV}86%	○ CF100%/RX_{UV}90%	○ CF100%/RX_{UV}86%
Film -forming	d	× CF75%/ RX_{UV}75%	× CF75%/RX_{UV}90%	○ CF100%/RX_{UV}89%	○ CF100%/RX_{UV}88%	○ CF99%/RX_{UV}90%
Film -forming	e	○ CF90%/ RX_{UV}84%	× CF15%/RX_{UV}112%	○ CF98%/RX_{UV}102%	○ CF100%/RX_{UV}85%	× CF5%/RX_{UV}70%
Penetrating	f	○ CF100%/RX_{UV}79%	○ CF100%/RX_{UV}79%	○ CF100%/RX_{UV}80%	○ CF100%/RX_{UV}83%	○ CF98%/RX_{UV}91%
Film -forming	g	○ CF98%/RX_{UV}82%	× CF0%/RX_{UV}46%	× CF15%/RX_{UV}85%	○ CF100%/RX_{UV}99%	× CF30%/RX_{UV}34%
Film -forming	h	○ CF100%/RX_{UV}85%	○ CF90%/RX_{UV}75%	× CF60%/RX_{UV}79%	○ CF100%/RX_{UV}83%	× CF70%/RX_{UV}59%

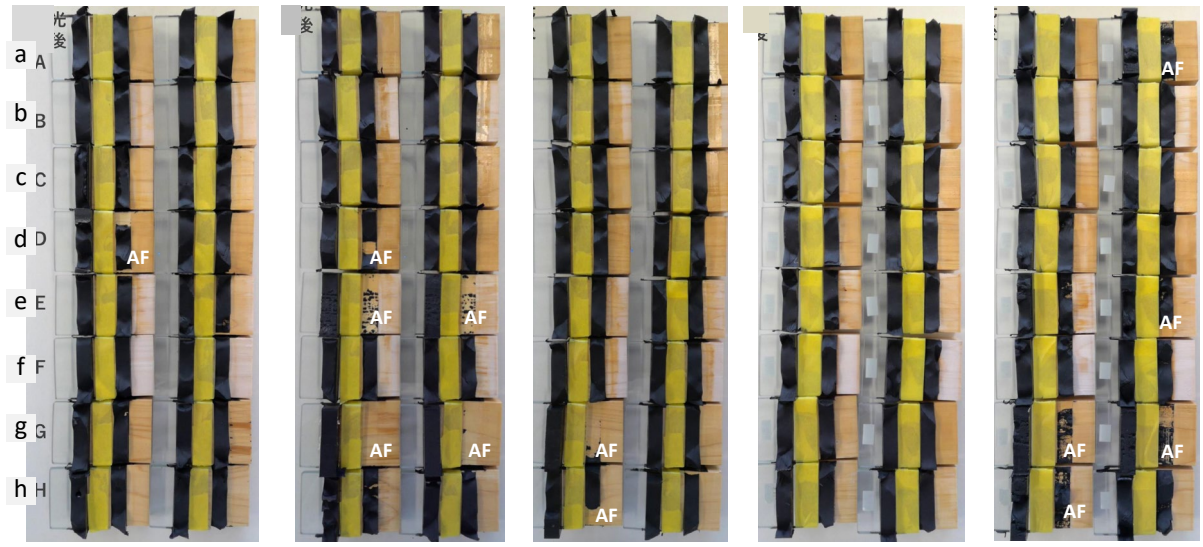

Fig. 12: Conditions of the specimens after testing (Artificial light exposure).

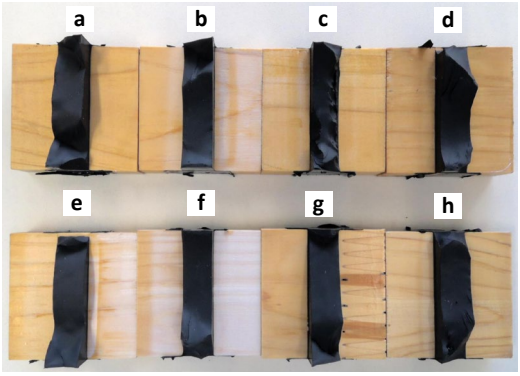

Fig. 13: Timber surface degradation after artificial light exposure.

In Chapter 4, the test protocols specified in JSIA 005 were conducted on Cypress glulam (glued laminated timber) to verify adhesion performance. The results confirmed that using appropriate primers and weather-resistant coatings, even timber-to-glass configurations can achieve excellent adhesion that satisfies the required performance values of JSIA 005, which were originally established for aluminum-to-glass applications.

5. Cyclic wind pressure test on the full-scale unit

Previously, adhesion was verified using small-scale specimens (50 mm x 50 mm). In this chapter, validation was performed through full-scale testing. As shown in Fig. 14, a full-scale timber SSG unit (GW2940 × GH805) was manufactured and installed in a wind pressure chamber. The unit was produced at the Sanshiba Shozai Co., Ltd. facility. The test involved applying a cyclic wind pressure of -1.15 kPa for 2.2 million cycles, followed by a final design wind pressure of -4.5 kPa in accordance with the loading diagram. With a unit height (GH) of 805 mm and a sealant width of 15 mm, the tensile stress generated at -1.15 kPa is 0.031 MPa. This corresponds to 22.2% of the design allowable tensile stress of 0.14 MPa typically used for SSG. At the design wind pressure of -4.5 kPa, the stress reached

86.3% of the allowable stress. The configuration utilized Cypress glulam (glued laminated timber), X-33-270-3 primer, and was left unpainted. Afterward, specimens were extracted from the unit using a water jet into the geometry shown in Fig. 15 for tensile testing to investigate the degree of degradation compared to the initial state. In accordance with JSIA 005, the loading rate (crosshead speed) was set to 50 mm/min. To facilitate the attachment of the tensile test jig, 12 mm thick plywood was bonded to the wood substrate using epoxy resin.

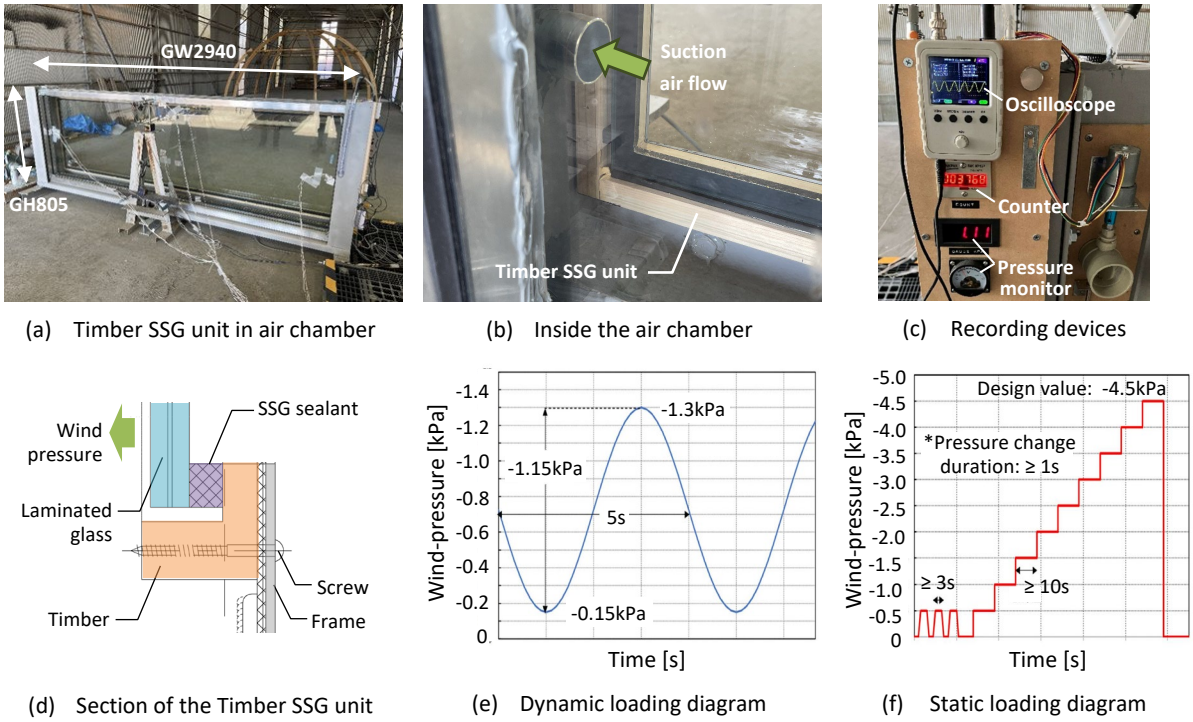

(a) Timber SSG unit in air chamber (b) Inside the air chamber (c) Recording devices

(d) Section of the Timber SSG unit (e) Dynamic loading diagram (f) Static loading diagram

Fig. 14: Outline of the cyclic wind pressure test.

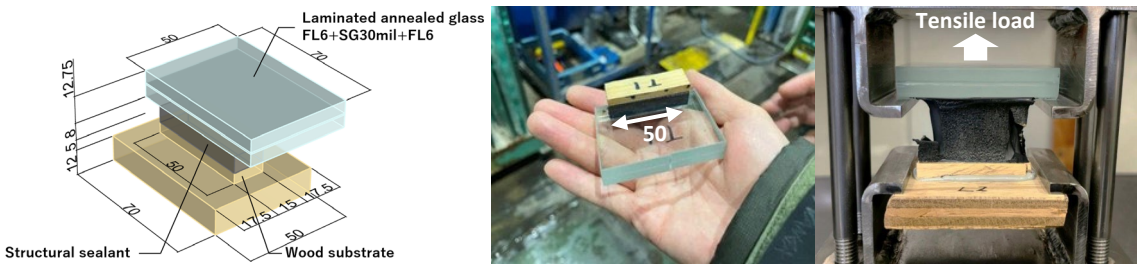

(a) The shape of the specimen (b) Specimen cut from the unit (c) During the tensile test

Fig. 15: Outline of the tensile specimen.

Fig. 16 illustrates the extraction positions of the specimens and screw joints, together with the corresponding test results. As shown in Fig. 16, the wind pressure acting on the glass is distributed to the areas T, B, R, and L and is borne by each edge. Therefore, the corner specimens were expected to be subjected to smaller loads, and specimens were cut out from different locations to examine these differences. In addition, as the screw pitch was set finely, the deflection of the timber was small, and the stress generated in the SSG sealant under wind pressure was considered to be uniformly distributed. The maximum tensile stress values ranged from 0.86 to 1.06 N/mm², with no significant variation observed based on the extraction position. The mean maximum tensile stress (X_{CL}) was 0.96 N/mm², and the residual strength ratio (RX_{CL})—calculated against the 23°C reference value X_{23}= 1.22

N/mm² from Section 4.1—was 78.7%. This demonstrates satisfactory adhesion that satisfies the JSIA 005 required performance values even after degradation.

However, as shown in Fig. 17, because the wood grain was parallel to the longitudinal direction of the SSG sealant, shear forces were generated in the sealant due to the "edge effect" mentioned by Pantaleo et al. (2012). This caused a phenomenon where the timber surface peeled from the edges along the fiber direction (grain orientation), and two specimens were confirmed to have a percentage of cohesive failure (CF) of less than 90%. To mitigate this, it is considered necessary to implement countermeasures such as ensuring proper edge treatment to prevent cracks or fissures during cutting, or avoiding sealant application to the very ends of the joints where such peeling is initiated.

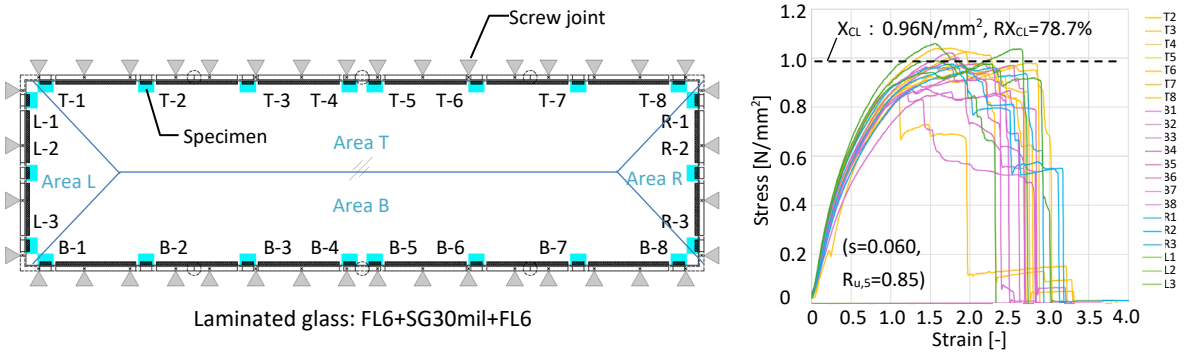

(a) Locations of specimens and screw joints

(b) Stress - strain curve

Fig. 16: Results of tensile tests after cyclic wind pressure.

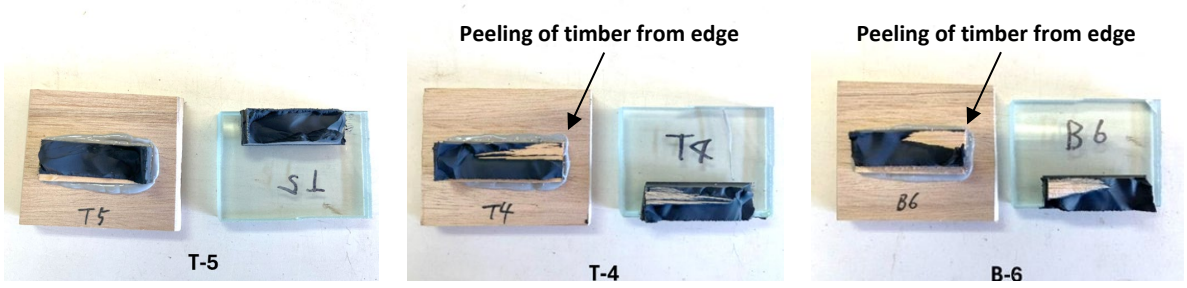

(a) T5 CF=100%

(b) T4 CF=80% (Timber failure 20%)

(c) B6 CF=80% (Timber failure 20%)

Fig. 17: Conditions of the specimens after testing.

6. Full scale mock-up

Finally, a full-scale mock-up was conducted. As shown in Fig. 18, three arch-shaped timber SSG units (maximum size GW2430 × GH2604) and one circular timber SSG unit (Φ1600) were manufactured. Fabrication was carried out at the Sanshiba Shozai Co., Ltd. facility. The timber SSG unit consists of a timber adapter frame with a 15 × 30 mm rectangular cross-section, CNC-machined to match the curved glass edges and bonded using a structural silicone sealant. These adapter frames are attached to the main timber frame using metal hardware and serve as the supporting edges that bear the wind pressure acting on the glass. The bonded SSG resists tensile forces during negative wind pressure (suction).

Cypress glulam (glued laminated timber) was used as the wood substrate. To compare the effects of aging under natural outdoor exposure, the primers X-33-270-3 and X-33-271 were applied separately

to each half of the units. Fig. 19 illustrates the workflow from factory fabrication to on-site installation. It was confirmed that CNC machining of the timber allows for the easy production and installation of timber SSG units, even when the edges feature complex free-form curves. This approach is considered capable of meeting the sophisticated design requirements made possible by the advancement of digital tools.

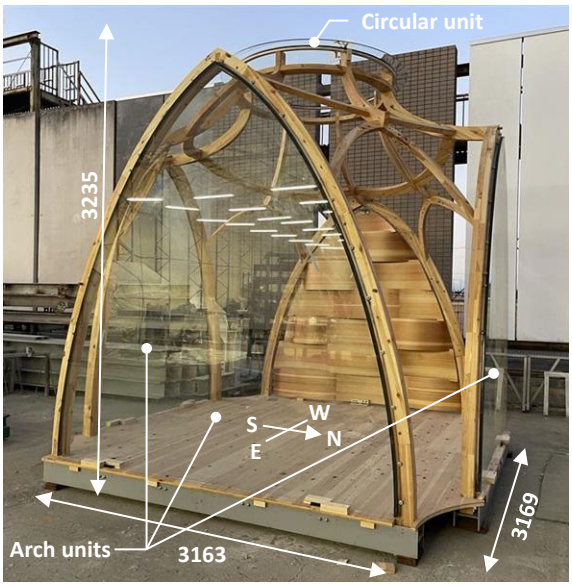

(a) Mock-up after installation of the SSG unit

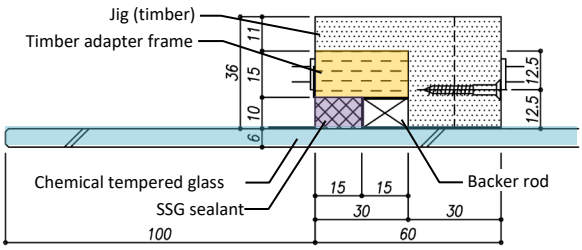

(b) Section of the circular unit during SSG application

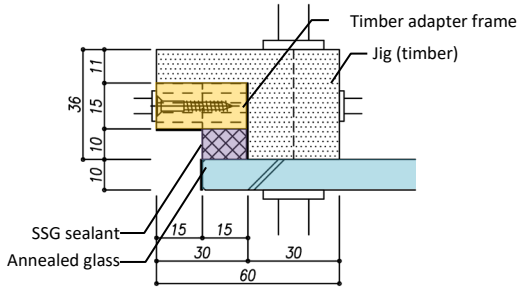

(c) Section of the arch unit during SSG application

Fig. 18: Outline of the mock-up.

(a) Applying the primer

(b) Applying SSG

(c) Installing a circular unit

(d) Installing arch units

Fig. 19: Process Flow: Fabrication to Installation of the timber SSG units.

7. Summary

In this study, the structural bonding performance between timber and glass was verified through both small-scale elemental tests and full-scale experimental testing. Furthermore, full-scale mock-ups were fabricated to evaluate the applicability of the system to actual building projects. The key findings obtained from this research are summarized below.

- H-piece tensile tests and S-piece shear tests were conducted on six different wood species; the results revealed that LVL (Cedar and larch) and Glulam (whitewood) exhibited wood failure (material failure) even in the initial state, indicating insufficient strength to support the sealant performance. Additionally, Glulam (Cedar and Scots pine) showed adhesive failure (AF) at the timber interface after immersion, which demonstrated insufficient adhesion. Conversely, Glulam (Cypress) frequently exhibited thin-layer cohesive failure (tCF) (near-surface cohesive failure) even after immersion, yielding the most promising results for potential application. Pantaleo et al. (2012) and Nicklisch et

al. (2016b) also reported that the bonding performance of SSG varies depending on the wood species.

- By improving the adhesive and film-forming components of the primer, the adhesion performance after hot water immersion could be enhanced. For Cypress glulam (glued laminated timber), 100% cohesive failure (CF) was ensured. Pantaleo et al. (2012) and Nicklisch et al. (2016b) also noted that applying a primer to the wood surface improves the bonding performance of SSG.
- Glass-to-glass H-piece specimens were enclosed in plastic bags along with wood pieces of five different species and subjected to hot water immersion. It was confirmed that wood extractives reduce the maximum tensile stress of the sealant, even without direct contact between the SSG sealant and the timber. Furthermore, in the case of thermally modified larch, a visual defect of sealant foaming (bubbling) was observed. Pantaleo et al. (2012) also reported adhesive failure at the wood–adhesive failure (AF) in pine, which is considered to be influenced by resin components present in the wood. In four-sided SSG systems, when the SSG bonding area is immersed in water due to condensation on the glass surface, a reduction in residual strength ratio and, depending on the timber species, surface defects may occur. Therefore, tensile tests after hot-water immersion are considered to be a useful method for evaluating such effects.
- A series of test protocols defined in JSIA 005 were conducted using Cypress glulam (glued laminated timber), and specifications that satisfy the required performance values were successfully obtained. In tensile tests following hot water immersion and artificial light exposure, eight types of transparent weather-resistant coatings were applied to verify their influence and effectiveness, leading to the identification of promising combinations.
- Cyclic wind pressure loading tests involving 2.2 million cycles were conducted on full-scale specimens. Subsequently, test pieces were extracted (cut out) from the unit and subjected to tensile tests. The results demonstrated sufficient residual strength, confirming the durability of the system.
- When the longitudinal direction of the sealant is parallel to the wood grain (fiber) direction, shear forces are applied to the timber ends due to the "edge effect" reported by Pantaleo et al. (2012), leading to a phenomenon where the timber surface peels off. To mitigate this, it is considered necessary to implement countermeasures such as ensuring proper edge treatment to prevent cracks or fissures during cutting, or avoiding sealant application to the very ends of the joints where such peeling is initiated. Serrano (2000) reported that the formation of a mechanically weak boundary layer (MWBL) on the wood surface during cutting results in a decrease in the strength of bonded joints, and Nicklisch et al. (2016b) highlighted the importance of planing.
- Full-scale mock-ups were fabricated, confirming that timber SSG units can be easily manufactured and installed even when the edges feature free-form curves. This demonstrates that the timber SSG construction method offers a high degree of design flexibility. Pantaleo et al. (2014) and Nicklisch et al. (2016a) have also conducted more practical studies with a view toward application in real construction projects.

Structural Sealant Glazing (SSG) systems in Japan experienced a hiatus of approximately 30 years from the late 1990s due to skepticism regarding adhesion performance; however, with the establishment of the JSIA 005 standard, the adoption of aluminum-to-glass SSG is now gradually increasing. While timber-to-glass SSG is still an emerging technology, the merits of utilizing wood are substantial in terms of environmental performance and resource efficiency, and it is hoped that this research will facilitate its wider adoption.

References

Architectural Institute of Japan (AIJ). (2003). JASS 17: Standard Specification for Glass Work. https://www.aij.or.jp/da1/detail.html?productId=625548

ASTM International. (2023). Standard Guide for Structural Sealant Glazing (ASTM C1401-23). https://doi.org/10.1520/C1401-23

ASTM International. (2019). Standard test method for determining tensile adhesion properties of structural sealants (ASTM C1135-19). https://doi.org/10.1520/C1135-19

Blyberg, L. (2011). "Timber/Glass Adhesive Bonds for Structural Applications". Licentiate thesis, Linnaeus University.

Choquet, Y. (2023). An Assessment of the Thermal Performance of Wood Curtain Wall Frames. Toronto Metropolitan University. Thesis. https://doi.org/10.32920/24033795.v1

European Organisation for Technical Assessment. (2018). Bonded glazing kits and bonding sealants (EAD 090010-00-0404). https://www.eota.eu/

European Organisation for Technical Approvals. (2012). Guideline for European technical approval for structural sealant glazing kits (ETAG) – Part 1: Supported and unsupported systems (ETAG 002-1). https://www.eota.eu/

Fadai, A., & Stephan, D. (2020). Conceptual design of timber-wood concrete-glass façades: A holistic approach. Challenging Glass 7. https://doi.org/10.7480/cgc.7.4481

Feldmann, M., Kasper, R., et al. (2014). " Guidance for European Structural Design of Glass Components ". JRC Scientific and Policy Reports. https://doi.org/10.2788/55303

ift Rosenheim. (2017). Beurteilungsgrundlage für geklebte Verglasungssysteme (ift-Richtlinie VE-08/4). https://www.ift-rosenheim.de/

Ishii, H., Matsuo, T., & Mori, H. (2013). Differences in standards and requirements for the application of four-sided structural sealant glazing (SSG) systems in Japan and other countries (materials and construction). Architectural Institute of Japan Annual Meeting, volume 83, 61–64, No.1016. (in Japanese) https://www.aij.or.jp/paper/detail.html?productId=413420

Ishii, H., Matsuo, T., Mori, H., Iwasaki, I., and Shimizu, Y. (2014). Investigation on guidelines for structural sealant glazing (SSG) systems in overseas countries: Part 3 – Design. Architectural Institute of Japan Annual Meeting, 1293–1294, No.1647. (in Japanese) https://www.aij.or.jp/paper/detail.html?productId=426259

Iwasaki, I., Matsuo, T., Ishii, H., Mori, H., and Shimizu, Y. (2014). Investigation on guidelines for structural sealant glazing (SSG) systems in overseas countries: Part 2 – Materials. Architectural Institute of Japan Annual Meeting, 1291–1292, No.1646. (in Japanese) https://www.aij.or.jp/paper/detail.html?productId=426258

Iwasaki, I., Matsuo, T., & Ishii, H. (2016). Survey on material standards for structural sealants in overseas countries. Architectural Institute of Japan Annual Meeting, 1369–1370, No.1685. (in Japanese) https://www.aij.or.jp/paper/detail.html?productId=375302

Iwasaki, I., Matsuo, T., Ishii, H., Shimizu, Y., Nishitani, K., Morimoto, H., Noguchi, O., Yamamoto, M., & Higaki, K. (2023). Test results according to specification plan for structural sealants: Part 2: Test results. Architectural Institute of Japan Annual Meeting, 1001-1002, No.1501. (in Japanese) https://www.aij.or.jp/paper/detail.html?productId=685799

Japanese Industrial Standards. (2013). JIS A 1415: Methods of exposure to laboratory light sources for polymeric material of buildings. Japanese Standards Association. (in Japanese) https://webdesk.jsa.or.jp/books/W11M0090/index/?bunsyo_id=JIS+A+1415%3A2013

Japanese Industrial Standards. (2022). JIS A 1439: Testing methods of sealants for sealing and glazing in buildings. Japanese Standards Association. (in Japanese) https://webdesk.jsa.or.jp/books/W11M0090/index/?bunsyo_id=JIS+A+1439%3A2022

Japanese Industrial Standards. (2008). JIS K 7350-2: Plastics — Methods of exposure to laboratory light sources — Part 2: Xenon-arc lamps. Japanese Standards Association. (in Japanese) https://webdesk.jsa.or.jp/books/W11M0090/index/?bunsyo_id=JIS+K+7350-2%3A2008

Japan Sealant Industry Association. (2025). JSIA 005: Standard test methods of sealants for structural glazing in buildings. Japan Sealant Industry Association. (in Japanese) https://www.sealant.gr.jp/book/kouzou

Matsuo, T., Ishii, H., Mori, H., Iwasaki, I., & Shimizu, Y. (2014). Investigation on guidelines for structural sealant glazing (SSG) systems in overseas countries: Part 1—Purpose and general rules. Architectural Institute of Japan Annual Meeting, 1289–1290, No.1645. (in Japanese) https://www.aij.or.jp/paper/detail.html?productId=426257

Matsuo, T., Ishii, H., Iwasaki, I., Shimizu, Y., Nishitani, K., Morimoto, H., Noguchi, O., Yamamoto, M., & Higaki, K. (2023). Test results according to specification plan for structural sealants: Part 1: Outline of trial test. Architectural Institute of Japan Annual Meeting, 999-1000, No.1500. (in Japanese)

https://www.aij.or.jp/paper/detail.html?productId=685798

Ministry of Construction of the People's Republic of China. (2003). JGJ 102-2003: Technical Code for Glass Curtain Wall Engineering. Beijing: China Architecture & Building Press. https://www.codeofchina.com/standard/JGJ102-2003.html

Nguyen, V. T., Gunalan, S., Woodfield, P., Doh, J.-H., Baker, M., & Stringfellow, J. (2026). Thermal performance of aluminium-timber composite frames in curtain wall systems. Energy and Buildings, 357, 117169. https://doi.org/10.1016/j.enbuild.2026.117169

Nicklisch, F., Dorn, M., Weller, B., & Serrano, E. (2014). "Joint study on material properties of adhesives to be used in load-bearing timber–glass composite elements". Engineered Transparency Conference, October 2014.

https://www.researchgate.net/publication/271824037

Nicklisch, F., & Weller, B. (2016a). "Adhesive bonding of timber and glass in load-bearing façades – evaluation of the ageing behaviour". World Conference on Timber Engineering, August 2016.

https://www.researchgate.net/publication/307174581

Nicklisch, F., Giese-Hinz, J., & Weller, B. (2016b). "Glued windows and timber-glass façades – performance of a silicone joint between glass and different types of wood". Engineered Transparency Conference, September 2016.

https://www.researchgate.net/publication/308416035

Pantaleo, A., Roma, D., & Pellerano, A. (2012). "Influence of wood substrate on bonding joint with structural silicone sealants for wood frame applications". International Journal of Adhesion & Adhesives, volume 37, September 2012, 121-128. https://doi.org/10.1016/j.ijadhadh.2012.01.017

https://www.sciencedirect.com/science/article/abs/pii/S0143749612000188

Pantaleo, A., Ferri, D., Roma, D., & Pellerano, A. (2013). Structural silicone sealant modelling for wood frames: influence of adhesion on bonding strength. Journal of Adhesion Science and Technology, 27(11), 1259–1277.

https://doi.org/10.1080/01694243.2012.737262

Pantaleo, A., Ferri, D., & Pellerano, A. (2014). Wooden window frames with structural sealants: manufacturing improvements and experimental validation of a finite element model. Journal of Adhesion Science and Technology, 28(2), 115–135. https://doi.org/10.1080/01694243.2013.827093

Serrano, E. (2000). "Adhesive Joints in Timber Engineering - Modelling and Testing of Fracture Properties". Doctoral Thesis, Lund University. https://portal.research.lu.se/files/4876529/5365311.pdf

Shimizu, Y., Matsuo, T., Ishii, H., Mori, H., and Iwasaki, I. (2014). Investigation on guidelines for structural sealant glazing (SSG) systems in overseas countries: Part 4 – Installation and maintenance. Architectural Institute of Japan Annual Meeting, 1295–1296, No.1648. (in Japanese) https://www.aij.or.jp/paper/detail.html?productId=426260

Challenging Glass Conference Proceedings – Volume 10 – June 2026 – Louter, Bos & Belis (Eds.)
International Conference on the Architectural and Structural Application of Glass
Challenging Glass Conference 10 – 15-17 June 2026 – TU Delft – The Netherlands

Platinum Sponsor

SAINT-GOBAIN

Gold Sponsors

EASTMAN

kuraray

NorthGlass®

sedak

seele

Silver Sponsors

DOW®

octatube

PERMASTEELISA GROUP

SEEN

Organisation

TU Delft

Technische Universität München

GHENT UNIVERSITY